Theory of the momentum flux probability distribution function for drift wave turbulence

Eun-jin Kim[a)] and P. H. Diamond
Department of Physics, University of California, San Diego, La Jolla, California 92093-0319

An analytical theory of the tails of the probability distribution function (PDF) for the local Reynolds stress (R) is given for forced Hasegawa–Mima turbulence. The PDF tail is treated as a transition amplitude from an initial state, with no fluid motion, to final states with different values of R due to nonlinear coherent structures in the long time limit. With the modeling assumption that the nonlinear structure is a modon (an exact solution of a nonlinear Hasegawa–Mima equation) in space, this transition amplitude is determined by an instanton. An instanton is localized in time and can be associated with bursty and intermittent events which are thought to be responsible for PDF tails. The instanton is found via a saddle-point method applied to the PDF, represented by a path integral. It implies the PDF tail for R with the specific form $\exp[-cR^{3/2}]$, which is a stretched, non-Gaussian exponential. © *2002 American Institute of Physics*. [DOI: 10.1063/1.1421616]

I. INTRODUCTION

For the last 40 years, much of the effort in magnetic fusion theory has been devoted to calculating turbulent heat and particle diffusivities for turbulence arising from various microinstabilities. A conventional approach to this problem is so-called mean field theory, which attempts to describe the transport by a single, average coefficient. It is, however, becoming increasingly clear that transport often involves events of many different amplitudes or scales, some of which are intermittent and bursty in time. In particular, recent numerical simulation[1] has indicated the existence of avalanche-like events of large amplitude, associated with coherent structures such as streamers or blobs, which can be major players in the transport dynamics. On the theory front, the notion of a scale invariant spectrum of transport events was proposed in self-organized criticality theory.[2] In short, it is evident that rather than a transport coefficient, the *flux probability distribution function (PDF) is required* in order to substantively characterize the transport process.

It is often found that PDF is Gaussian near its center but reveals a significant deviation from Gaussianity at the tails.[3] The latter is a manifestation of *intermittency* due to rare events of substantial amplitude, which are frequently associated with bursts and coherent structures. That is, the events contributing to the tails are intrinsically strongly nonlinear. Thus, unlike near the center of PDF, where a perturbative approach may be useful, a nonperturbative approach is required for the description of PDF tails. Unfortunately, little in the way of intuition concerning PDF structure is available. Moreover, since numerical calculation of PDFs (via repeated simulations) is slow and costly, a (nonperturbative) analytical theory is especially useful.

In this paper, we take a novel statistical approach and provide an analytical theory for the prediction of the tails of local Reynolds stress (vorticity flux) PDF in drift wave turbulence. We consider forced Hasegawa–Mima turbulence[4] as the simplest description of drift wave turbulence and study momentum transport by computing the PDF for local Reynolds stress (i.e., momentum flux). Note that the issue of particle or heat transport, which is of our ultimate interest, cannot be addressed in the Hasegawa–Mima model and requires consideration of a more complicated model such as Hasegawa–Wakatani,[5] ion temperature gradient turbulence[6] (ITG), or dissipative trapped ion convective cell (DTICC)[7] models.

As noted previously, PDF tails are likely to arise from events with coherent spatial structure. One of the coherent structures manifested in a particular system is obviously an exact solution of the governing nonlinear equation. In the case of the Hasegawa–Mima equation, one exact solution is known as a modon.[8] This is a bipolar vortex soliton, which is localized in space and travels in the direction perpendicular to both the (strong) magnetic field and the background density gradient. Being a solitary solution in the absence of dissipation and an external forcing, a modon can be excited/generated in finite time by the proper forcing. Here, what we meant by "proper" is that a forcing should be somewhat fine-tuned to excite modons as a result of *resonant* interaction (see Sec. III). The key idea is then to envision the tails of the local Reynolds stress PDF as the transition amplitude from an initial state, with no fluid motion, to final states with different values of local Reynolds stresses owing to the presence of a modon in the long time limit.

As shall be shown in Sec. II, a PDF can, in general, be expressed in terms of a path integral, by exploiting the uncertainty arising due to an external, stochastic forcing.[9,10] The path integral can then be performed nonperturbatively by computing the saddle-point solution for the effective action. The saddle-point solution for a dynamical variable $u(\mathbf{x},t)$ of the form $u(\mathbf{x},t)=F(t)u_0(\mathbf{x})$ is called an instanton if $F(t)=0$ at the initial time and $F(t)\neq0$ in the long time limit.[11–13] Here, $u_0(\mathbf{x})$ represents a spatial pattern of a coherent structure. Among all possible paths contributing to a
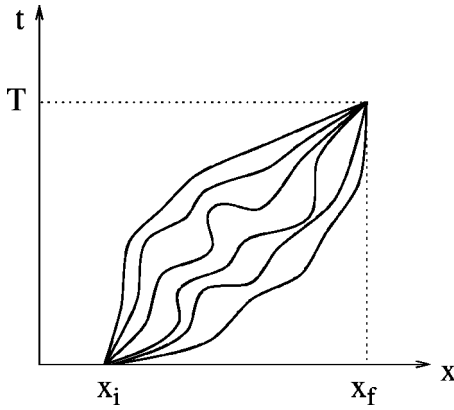
FIG. 1. Trajectories of a particle between initial position x_i at time $t=0$ and final position x_f at $t=T$.

FIG. 2. (a) The double-well potential with a particle sitting at the bottom of potential well. A particle going from $x=-a$ to a is called an instanton while the one going from $x=a$ to $-a$ is an anti-instanton. (b) The position of a particle as a function of time, which travels between $x=-a$ and a. The positive (negative) slope corresponds to instanton (anti-instanton).

PDF, an instanton corresponds to a particular path which determines the PDF tail in such a way as to give the transition amplitude mentioned previously. As the name indicates, an instanton is localized in time with a kink-like structure [see Fig. 2(b) below] and exists during the time interval while a modon is formed by forcing. Thus, its finite lifetime can be related to the burstiness of the event associated with the creation of a modon.

In principle, the computation of the true PDF tail (thus, intermittency) requires a weighted sum over various coherent structures. Note that the notion of a weighted sum over different coherent structures in real space (rather than conventional Fourier expansion) is employed here. In the present paper, however, we shall assume that underlying coherent structure is a modon as it is the only nonlinear solution that is known to us. The generalization to the case with many different coherent structures is expected to be straightforward, even if technically complicated. Note that the incorporation of other coherent structures may alter the scaling of the PDF tails.

Before closing the introductory remarks, some historical background on instantons would be helpful in understanding their physical meaning. Instantons originated in quantum mechanics as a nonperturbative way of computing the transition amplitude from one ground state to another.[14] The basic idea there is that the uncertainty relation between position and momentum allows one to formulate the transition amplitude from the initial position x_i to final position x_f by a path integral as follows (see Fig. 1):

$$\langle x_f | e^{iHT/\hbar} | x_i \rangle = N \int_{x=x_i}^{x=x_f} \mathcal{D}x(t) e^{iS/\hbar},$$

where $S = \int dt[mv^2/2 - U(x)]$ is action, and $H = mv^2/2 + U(x)$ is Hamiltonian with a potential U. We can expand the left-hand side of the previous equation in terms of a complete set of energy eigenstates to obtain

$$\langle x_f | e^{iHT/\hbar} | x_i \rangle = \sum_n \langle x_f | E_n \rangle \langle E_n | x_i \rangle e^{iE_n T/\hbar}.$$

The previous equation then implies that the transition amplitude from one ground state to another can be isolated by taking time to be imaginary. Expressed in terms of imaginary
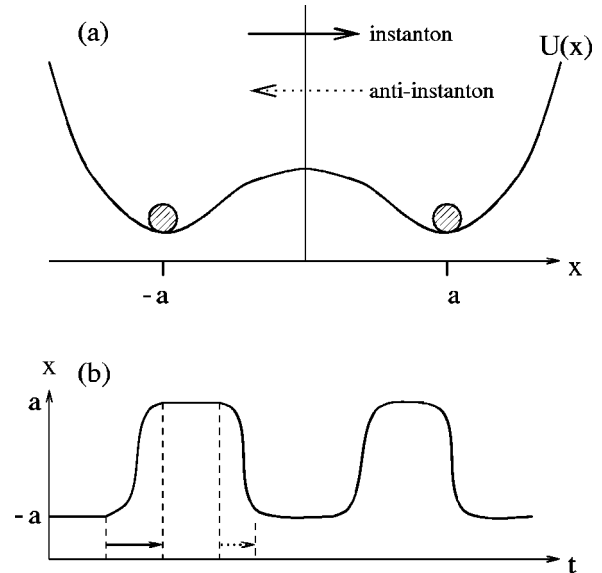
time, action becomes "Euclidean" action, $S_E = \int dt[mv^2/2 + U]$. An instanton is a saddle-point solution of Euclidean action and corresponds to one particular path which leads to the transition amplitude between ground states. For instance, in the case of double-well potential, an instanton is a tunneling solution from the bottom of one potential well to another [see Fig. 2(a)]. If a solution going from one ground state to the other is called instanton, a solution traveling in the opposite direction is called anti-instanton. As noted previously, a distinguishing characteristic of such solutions is temporal localization [see Fig. 2(b)]. The instanton method was used in gauge field theory for the computation of the transition amplitude from one vacuum to another vacuum.[15] About 20 years later, this method was adapted to a classical fluid problem by several authors.[11–13,16]

In fluid turbulence, unpredictability can arise either from the chaos intrinsic to the system or from an external random forcing. Between the two, clearly, it is much easier to formulate a PDF in the case of an external forcing, to which the following discussion will be limited. In fact, it is well known that a similar path integral can be formulated for stochastic equations with a random external forcing.[9,10] For instance, the effective action for classical forced systems was formulated by Martin, Sigga, and Rose in 1973.[17] However, the nonperturbative evaluation of a path integral had to wait until when the (nonperturbative) saddle-point (instanton) method was adopted in the computation of the tail of the PDF.[12,11] Let us discuss briefly how this was done in Burgers turbulence.

Burgers turbulence is bifractal, i.e., there are two different coherent structures, namely shocks and ramps. While shocks (with negative slope), leading to the negative velocity difference, contribute to the left tails of PDF, ramps (with positive slope) determine the right tails of PDF. Since negative/positive slopes amplify/flatten due to the nonlinear

advection, PDF for the velocity difference exhibits the asymmetry between left and right tails. By making an ansatz that an instanton is a temporally localized ramp, i.e., $u_{int} = F(t)x$, Gurarie and Migdal[11] computed the right tail of PDF for the case of a simple Gaussian forcing, which is delta correlated in time with a smooth variation in space. The instanton (saddle-point) solution they found yields the right tail of PDF for velocity difference Δu of the form $\exp\{-\alpha \Delta u^3\}$, which is a non-Gaussian exponential. Here, α is a constant. It turns out that the prediction of the left tail of the PDF is much more difficult because of the small scale structure of shocks, where the viscosity plays a major role.

The difficulty of computing the PDF tail arising from a small-scale coherent structure, such as shocks, is one of the major shortcomings of an instanton method, at least at the present time. The other limitation of this method is that to leading order, it is likely to lead to exponential PDF tails. It is because, to leading order, the PDF tails are determined by the evaluation of saddle-point action. Thus, this method may not be utilized for power-law PDF tails. Nevertheless, it is a powerful nonperturbative method for calculations of PDF tails, and shall be employed here to gain some understanding of PDF tails for local Reynolds stress in drift wave turbulence.

The rest of the paper is organized as follows. In Sec. II, we provide a path integral formulation for local Reynolds stress PDF in Hasegawa–Mima turbulence. The PDF tail is computed via an instanton solution in Sec. III. Our discussion and conclusions are found in Sec. IV. Section V is devoted to comments on the instanton method.

II. PDF FOR LOCAL REYNOLDS STRESS IN FORCED HASEGAWA–MIMA TURBULENCE

As a simple model for drift wave turbulence, we adopt the forced Hasegawa–Mima equation,[4] by assuming cold ions and adiabatic electrons in a slab geometry:

$$(1-\nabla^2)\partial_t\phi + v_*\partial_y\phi - \mathbf{v}\cdot\boldsymbol{\nabla}\nabla^2\phi = f. \qquad (1)$$

Here x and y denote local radial and poloidal direction, respectively, and $\nabla^2 = \partial_x^2 + \partial_y^2$; $v_* = \rho_s^2\Omega_i/L_n$ is the drift velocity due to radial density gradient; $L_n = -(\partial_x n_0/n_0)^{-1}$ is the (background) density length scale; $\rho_s^2 = T_e/(m_i\Omega^2)$ where T_e, m_i, and Ω_i are electron temperature, ion mass, and ion gyrofrequency; ϕ, $\mathbf{v} = -\boldsymbol{\nabla}\times\phi\hat{z}$, and f are the electric potential, $\mathbf{E}\times\mathbf{B}$ advection velocity, and external forcing.

Note that Eq. (1) is non-dimensionalized by measuring the length, velocity, and ϕ in units of ρ_s, c_s, and T_e/e where c_s is sound speed.

A. Gaussian statistics of forcing

For simplicity, we shall take the statistics of the forcing to be Gaussian with delta correlation in time as follows:

$$\langle f(\mathbf{x},t)f(\mathbf{x}',t')\rangle = \delta(t-t')\kappa(\mathbf{x}-\mathbf{x}'), \qquad (2)$$

and $\langle f\rangle = 0$. Here, the temporal delta correlation was assumed for the simplicity of the analysis. In the case of a forcing with a finite correlation time, one would need to solve nonlocal integral equations in time. For Gaussian statistics with vanishing first moment, the prescription of the second moment given by Eq. (2) is sufficient. It is simply because all odd moments vanish while even moments can be expressed as a product of second moments. Note that even if the forcing is Gaussian, statistics of ϕ can be non-Gaussian because of the nonlinearity of the dynamical equation. An equivalent way of prescribing the second moment (2) for the Gaussian forcing is to introduce the probability density function for f as follows:[10]

$$d[\rho(f)] = \mathcal{D}f \exp\left\{ -\frac{1}{2}\int d\mathbf{x}\,d\mathbf{x}'\,dt \right.$$
$$\left. \times f(\mathbf{x},t)\kappa^{-1}(\mathbf{x},\mathbf{x}')f(\mathbf{x}',t) \right\}. \qquad (3)$$

This is a generalization of Gaussian distribution to a continuous variable $f(\mathbf{x},t)$. The average value of a quantity Q is then computed as

$$\langle Q\rangle = \int d[\rho(f)]Q.$$

For instance, by taking $Q = f(\mathbf{x},t)f(\mathbf{x}',t')$, one can easily reproduce Eq. (2).

When the average value of a functional of ϕ (i.e., $\langle Q[\phi]\rangle$) is required, the constraint should be imposed that f and ϕ satisfy the original equation (1). This can be done by inserting an identity with a delta function, which enforces Eq. (1), as

$$N = \int \mathcal{D}\phi\,\delta[(1-\nabla^2)\partial_t\phi + v_*\partial_y\phi - \mathbf{v}\cdot\boldsymbol{\nabla}\nabla^2\phi - f], \quad (4)$$

where N is a number arising from the Jacobian due to the change of integral variables.[10,11] Let us show in detail how this is done. Starting from the definition,

$$\langle Q[\phi]\rangle = \int \mathcal{D}f Q[\phi] \exp\left\{ -\frac{1}{2}\int d\mathbf{x}\,d\mathbf{x}'\,dt\,f(\mathbf{x},t)\kappa^{-1}(\mathbf{x},\mathbf{x}')f(\mathbf{x}',t) \right\}$$

$$\simeq \int \mathcal{D}f\mathcal{D}\phi Q[\phi]\delta[(1-\nabla^2)\partial_t\phi - v_*\partial_y\phi + \mathbf{v}\cdot\boldsymbol{\nabla}\nabla^2\phi - f] \exp\left\{ -\frac{1}{2}\int d\mathbf{x}\,d\mathbf{x}'\,dt\,f(\mathbf{x},t)\kappa^{-1}(\mathbf{x},\mathbf{x}')f(\mathbf{x}',t) \right\}$$

$$\simeq \int \mathcal{D}f\mathcal{D}\phi\mathcal{D}\bar{\phi}Q[\phi] \exp\left\{ i\int d\mathbf{x}\,dt\,\bar{\phi}[(1-\nabla^2)\partial_t\phi + v_*\partial_y\phi - \mathbf{v}\cdot\boldsymbol{\nabla}\nabla^2\phi - f] \right\}$$

$$\times \exp\left\{ -\frac{1}{2}\int d\mathbf{x}\,d\mathbf{x}'\,dt\,f(\mathbf{x},t)\kappa^{-1}(\mathbf{x},\mathbf{x}')f(\mathbf{x}',t) \right\}$$

$$= \int \mathcal{D}\phi\mathcal{D}\bar{\phi}Q[\phi]e^{-S}, \qquad (5)$$

where

$$S = -i \int d^2x \, dt \, \bar{\phi}[(1-\nabla^2)\partial_t \phi + v_* \partial_y \phi - \mathbf{v} \cdot \nabla \nabla^2 \phi]$$

$$+ \frac{1}{2} \int d^2x \, d^2x' \, dt \, \bar{\phi}(\mathbf{x},t)\kappa(\mathbf{x}-\mathbf{x}')\bar{\phi}(\mathbf{x}',t). \qquad (6)$$

Here N is dropped,[10,11] and the functional Gaussian integral over f was performed to obtain the last line of Eq. (5). Note that $\bar{\phi}$ is a conjugate variable, which acts as a mediator between the forcing κ and dynamical variable ϕ.

B. PDF for local Reynolds stress

We now construct PDF for local Reynolds stress $\langle v_x v_y(\mathbf{x}_0)\rangle = \langle -\partial_x \phi \partial_y \phi(\mathbf{x}_0)\rangle$ in terms of a path integral, by utilizing the probability density function for the Gaussian forcing equation (3) and Eqs. (5) and (6). Here, the angular brackets denote the average over the statistics of the forcing. By definition, the probability distribution function for local Reynolds stress at point $\mathbf{x}_0$ to take a value R is

$$P(R;\mathbf{x}_0) = \langle \delta(v_x v_y|_{\mathbf{x}_0} - R)\rangle$$

$$= \int d\lambda \, e^{i\lambda R}\langle e^{-i\lambda(v_x v_y)(\mathbf{x}=\mathbf{x}_0)}\rangle$$

$$= \int d\lambda \, e^{i\lambda R} I_\lambda, \qquad (7)$$

where

$$I_\lambda = \langle e^{-i\lambda(v_x v_y)(\mathbf{x}=\mathbf{x}_0)}\rangle.$$

By taking $Q[\phi] = \exp[-i\lambda v_x v_y(\mathbf{x}_0)]$ in Eq. (5), I_λ can be rewritten in terms of a path integral as

$$I_\lambda = \int \mathcal{D}\phi \mathcal{D}\bar{\phi} \, e^{-S_\lambda}. \qquad (8)$$

Here S_λ is the effective action given by

$$S_\lambda = -i \int d^2x \, dt \, \bar{\phi}[(1-\nabla^2)\partial_t \phi + v_* \partial_y \phi - \mathbf{v} \cdot \nabla \nabla^2 \phi]$$

$$+ \frac{1}{2} \int d^2x \, d^2x' \, dt \, \bar{\phi}(\mathbf{x})\kappa(\mathbf{x}-\mathbf{x}')\bar{\phi}(\mathbf{x}')$$

$$+ i\lambda \int d^2x \, dt(-\partial_x \phi \partial_y \phi)\delta(t)\delta(\mathbf{x}-\mathbf{x}_0). \qquad (9)$$

Equation (8) is the path integral representation of the PDF that we have been seeking.

III. INSTANTON (SADDLE-POINT) SOLUTION AND PDF TAILS

So far, we have just shifted the problem of computing the PDF in Eq. (7) to the computation of a path integral in Eq. (8). Although this path integral cannot be calculated exactly in general, it can be evaluated approximately in the limit of $\lambda \to \infty$ by a saddle-point method. That is, in the limit of $\lambda \to \infty$, the leading order contribution to the integral of $\exp[-S_\lambda]$ comes from a particular path which satisfies saddle-point equations

$$\frac{\delta S_\lambda}{\delta \phi} = 0, \quad \frac{\delta S_\lambda}{\delta \bar{\phi}} = 0. \qquad (10)$$

What then is the meaning of the parameter λ and when can it be taken to be large? In order to answer these questions, we first notice that the evaluation of PDF in Eq. (7) requires the integral over λ once I_λ is computed by the saddle-point method. As we are interested in the large R limit for PDF tails, we can compute the λ integral in Eq. (7) by applying the saddle-point method once more. For example, let us assume that $I_\lambda \sim \exp[-S_\lambda(0)]$ with $S_\lambda(0) = i\alpha\lambda^n$, where $S_\lambda(0)$ is the saddle-point action due to an instanton solution, and α and n are constants. Then, the saddle point for the integrand of Eq. (7) satisfies $\partial_\lambda(\lambda R - \alpha\lambda^n) = 0$, i.e., $\lambda \propto R^{1/(n-1)}$. This is the very relation between the parameter λ and physical quantity R and indicates that the limit of $R \to \infty$ ensures the $\lambda \to \infty$ limit when $n > 1$. Thus, λ can be taken to be large if $n > 1$. In the following, we shall assume λ to be a large parameter to begin with and then check the validity of this assumption after computing I_λ in Eq. (8).

It, however, turns out that the direct application of the saddle-point method results in very complicated partial differential equations for ϕ and $\bar{\phi}$. For this reason, we opt to substitute the ansatz that the saddle-point solution (instanton) is a temporally localized modon, i.e.,

$$\phi(\mathbf{x},t) = \psi(\mathbf{x},t)F(t), \qquad (11)$$

in S_λ before minimizing it. Here $\psi(\mathbf{x},t) = \psi(x,y-Ut)$ is a modon solution given by

$$\psi(x,y-Ut) = [c_1 J_1(kr) + (\beta - k^2 U)r/k^2]\cos\theta,$$
$$\text{for } r < a, \qquad (12)$$

$$\psi(x,y-Ut) = c_2 K_1(pr)\cos\theta, \quad \text{for } r > a,$$

where $r = \sqrt{x^2 + y'^2}$, $\tan\theta = y'/x$, $y' = y - Ut$, $\beta = v_* - U$, $p^2 = -\beta/U$, $c_1 = -\beta a/k^2 J_1(ka)$, $c_2 = -Ua/K_1(pa)$, and $J_1'(ka)/J_1(ka) = (1+k^2/p^2)/ka - kK_1'(pa)/pK_1(pa)$; U is the velocity of a modon; a is the size of the core region; J_1 and K_1 are the first Bessel and the second modified Bessel functions.

A modon is an exact solution of the Hasegawa–Mima equation in the absence of dissipation and an external forcing. It is a bipolar vortex soliton, which is spatially localized in the frame moving with a velocity $U\hat{y}$, and has no net angular momentum. In physical terms, we are expecting the coherent structure contributing to PDF tails to be modons which are created by the external forcing, thereby acquiring the time dependence $F(t)$ in Eq. (11). As noted in Sec. I, PDF tails are then interpreted as the transition amplitude going from the state with no fluid motion to final states with different values of local Reynolds stresses due to different amplitude of modons. The time variation of ϕ, i.e., $F(t)$, can be associated with the degree of burstiness of an event.

Once the ansatz for the instanton (11) is substituted in Eq. (9), the spatial integral in S_λ can be performed formally as follows. First, we prescribe the spatial form of correlation function to be approximately parabolic for $|\mathbf{x}-\mathbf{x}'| < L$ and to vanish for $|\mathbf{x}-\mathbf{x}'| > L$. That is,

$$\kappa(\mathbf{x}-\mathbf{x}')=\kappa_0 J_0(k_f|\mathbf{x}-\mathbf{x}'|)\quad\text{for }|\mathbf{x}-\mathbf{x}'|<L,\qquad(13)$$

where $L\lesssim\alpha_{01}/k_f$ with α_{01} being the first zero of J_0. Note that J_0 is chosen to simplify the following analysis. Second, owing to the completeness of Bessel and Fourier series, the conjugate variable can be expanded in the following form:

$$\bar{\phi}(r<a,\theta,t)=\sum_{m,n}J_m\left(\frac{\alpha_{mn}}{a}r\right)$$
$$\times[a_{mn}(t)\sin m\theta+b_{mn}(t)\cos m\theta],$$
$$(14)$$
$$\bar{\phi}(r>a,\theta,t)=\sum_{m,n}K_m(q_{mn}r)$$
$$\times[\bar{a}_{mn}(t)\sin m\theta+\bar{b}_{mn}(t)\cos m\theta],$$

where $a_{mn}(t)$, $b_{mn}(t)$, $\bar{a}_{mn}(t)$, and $\bar{b}_{mn}(t)$ are unknown functions of time, which are to be determined by saddle-point equations.

The substitution of Eqs. (11)–(14) in (9) now reduces S_λ to an integral with respect to time only with the form

$$S_\lambda=-i\int dt\sum_n[\dot{F}(\bar{A}_n\bar{b}_{1n}+A_nb_{1n})+F(F-1)B_na_{2n}]$$
$$+\kappa_0\int dt\sum_{m,n}[(D_nb_{1n}+\bar{D}_n\bar{b}_{1n})(D_mb_{1m}+\bar{D}_m\bar{b}_{1m})$$
$$+E_mE_na_{2m}a_{2n}]+i\lambda\int dt\,F^2\xi_0\delta(t).\qquad(15)$$

Here

$$\xi_0=-\partial_x\psi\partial_y\psi(\mathbf{x}=\mathbf{x}_0),$$

$$A_n=\frac{1}{2}c_1(1+k^2)\int_0^a dr\,rJ_1(kr)J_1(\alpha_{1n}r/a)$$
$$+\frac{\alpha}{2k^2}\int_0^a dr\,r^2J_1(\alpha_{1n}r/a),$$

$$B_n=-\frac{k\alpha}{4}\int_0^a dr\,rJ_2(kr)J_2(\alpha_{2n}r/a),$$

$$D_n=\frac{1}{2}\int_0^a dr\,rJ_1(k_fr)J_1(\alpha_{1n}r/a),$$

$$E_n=\frac{1}{2}\int_0^a dr\,rJ_2(k_fr)J_2(\alpha_{2n}r/a),$$

$$\bar{A}_n=\frac{1}{2}c_2(1-p^2)\int_a^L dr\,rK_1(q_{1n}r)K_1(pr),$$

$$\bar{D}_n=\frac{1}{2}\int_a^L dr\,rK_1(q_{1n}r)J_1(k_fr),$$

where $\alpha=\beta-k^2U$; α_{in} is nth zero of J_i [i.e., $J_i(\alpha_{in})=0$]; q_{1n} is a constant. In obtaining Eq. (15), we used the expansion of J_0 for a small argument as

$$J_0(k_f|\mathbf{x}-\mathbf{x}'|)\sim J_0(k_fr)J_0(k_fr')$$
$$+2J_1(k_fr)J_1(k_fr')\cos(\theta-\theta')$$
$$+2J_2(k_fr)J_2(k_fr')\cos2(\theta-\theta')+\cdots.$$

We note that coefficients A_n, $\bar{A}_n$, and B_n involve the projection of the conjugate variable onto the modon, while D_n, $\bar{D}_n$, and E_n contain the projection of the forcing onto conjugate variable. As shall become clear in Sec. III A, nonvanishing value for both sets of coefficients, accordingly nonvanishing projection of the forcing onto modon itself, is necessary for the existence of a nontrivial solution for F. This projection is likely to be maximized by choosing the characteristic scale of the forcing to be comparable to that of a modon, i.e., when $k_f\sim k$. Furthermore, note that A_n, D_n, $\bar{A}_n$, and $\bar{D}_n$ originate from the terms involving $\cos\theta$ while B_n and E_n from those with $\sin2\theta$. That is, the (spatial) "overlap" between the forcing and modon is critical for the generation of the modon. This is what we meant by fine-tuning of a forcing or "resonant" generation of a modon by a forcing in Sec. I. In more general terms, which coherent structure is likely to be generated is determined by a forcing, with different forcings giving rise to different intermittency.

Since $F(t)$, $a_{mn}(t)$, $b_{mn}(t)$, $\bar{a}_{mn}(t)$, and $\bar{b}_{mn}(t)$ are independent variables, S_λ should be minimized with respect to these variables to obtain saddle-point equations. This minimization will lead to coupled equations among $F(t)$, $a_{mn}(t)$, $b_{mn}(t)$, $\bar{a}_{mn}(t)$, and $\bar{b}_{mn}(t)$, which are ordinary differential equations (ODEs) for time t, rather than partial differential equations. Thus, the advantage of using ansatz (11) as well as Eqs. (13) and (14) was to put saddle-point equations in the form of ODEs, which are much easier to solve. In Secs. III A and III B, solutions for these saddle-point equations (i.e., instantons) will be provided, together with the corresponding saddle-point action and PDF tail.

A. Instanton solutions

The saddle-point equations for instantons are obtained by minimizing the effective action S_λ with respect to independent variables $F(t)$, $a_{mn}(t)$, $b_{mn}(t)$, $\bar{a}_{mn}(t)$, and $\bar{b}_{mn}(t)$. Most of these equations turn out to be trivial, simply giving vanishing values for many of variables. The nontrivial saddle-point equations are for a_{2n}, b_{1n}, $\bar{b}_{1n}$, and F, which take the following forms:

$$-iA_n\partial_tF+2\kappa_0\sum_m(D_mb_{1m}+\bar{D}_m\bar{b}_{1m})D_n=0,\qquad(16)$$

$$-iB_nF(F-1)+2\kappa_0\sum_m E_nE_ma_{2m}=0,\qquad(17)$$

$$-i\bar{A}_n\partial_tF+2\kappa_0\sum_m(D_mb_{1m}+\bar{D}_m\bar{b}_{1m})\bar{D}_n=0,\qquad(18)$$

$$\sum_n[A_n\partial_tb_{1n}+\bar{A}_n\partial_t\bar{b}_{1n}-B_n(2F-1)a_{2n}]$$
$$=-2\lambda F(t)\delta(t)\xi_0.\qquad(19)$$

Equation (19) indicates that there is a singularity at time $t=0$. To give a proper meaning to this singularity, it is important to realize that physical quantity $F(t)$ should be a smoothly varying function of time. The inspection of Eqs. (16)–(19) then tells us that the singularity should come from $\partial_t b_{1n}$ and $\partial_t \bar{b}_{1n}$. That is, b_{1n} and $\bar{b}_{1n}$ have discontinuity at $t=0$. Furthermore, we note that the incorporation of a small viscosity will lead to saddle-point equations for the conjugate variables which have a negative viscosity (see Ref. 11). In other words, conjugate variables propagate backward in time. Thus, $b_{1n}=0$, $\bar{b}_{1n}=0$, and $a_{2n}=0$ for $t\geq 0$. In view of the role of conjugate variables mediating between forcing and F, conjugate variables vanishing at $t\geq 0$ can be interpreted as a "causality" condition, requiring the forcing to precede the correlation function (PDF) that we are interested in. With the help of these observations, we now integrate Eq. (19) for a small time interval $t\in[-\epsilon,0]$ ($\epsilon\ll 1$) to obtain the relation, at $t=-\epsilon$,

$$\sum_n [A_n b_{1n} + \bar{A}_n \bar{b}_{1n}] = 2\lambda F_0 \xi_0, \tag{20}$$

where $F_0 = F(t=0)$.

For $t<0$, the coupled equations (16)–(19) can be combined to give an equation for F as

$$\partial_{tt} F - \gamma(F^2 - F)(2F-1) = 0, \tag{21}$$

where

$$\gamma = \frac{B^2/E^2}{Q}, \quad Q = \frac{A^2}{D^2} = \frac{\bar{A}^2}{\bar{D}^2},$$

with $B^2 = \sum_m B_m B_m$, $A^2 = \sum_m A_m A_m$, $D^2 = \sum_m D_m D_m$, and $\bar{D}^2 = \sum_m \bar{D}_m \bar{D}_m$. Equation (21) is to be solved by using that $F(t)=F_0$ at $t=0$ and $F(t)=0$ as $t\to-\infty$. The latter is imposed because the instanton is expected to capture the formation process of a modon. Here, the value of F_0 can be found by plugging Eqs. (16) and (18) in (20). A solution satisfying these conditions is

$$F(t) = \frac{1}{1 - \dfrac{F_0 - 1}{F_0} \exp\{-\sqrt{\gamma}t\}}, \tag{22}$$

where

$$F_0 = 1 + \frac{i4\kappa_0 \lambda}{\sqrt{\gamma}Q}\xi_0.$$

The instanton solution (22) is localized within a time interval proportional to $1/\sqrt{\gamma}$. Note that λ appearing in F_0 is a parameter that is assumed to be large. It will be related to a physical quantity R in Sec. III B.

B. PDF tails

Having found the saddle-point solution, it is straightforward to calculate the value of S_λ at saddle point (i.e., saddle-point action) by using Eqs. (16)–(18) and (22) in (15). To leading order in λ, it can easily be shown that

$$S_\lambda \simeq -\frac{i}{3}h\lambda^3, \tag{23}$$

where

$$h = \xi_0^3 q^2, \quad q = \left| \frac{4\kappa_0}{\sqrt{\gamma}Q} \right|.$$

PDF tails for local Reynolds stress R can now be computed by doing λ integral in Eq. (7) by the saddle-point method. In the case where $R/\xi_0 > 0$, the saddle point satisfies $\lambda \xi_0 q = i(R/\xi_0)^{1/2}$, leading to the following PDF tail:

$$P(R;\mathbf{x}_0) \sim \exp\left\{ -\frac{2}{3q}\left(\frac{R}{\xi_0}\right)^{3/2} \right\}. \tag{24}$$

Note that the saddle-point solution justifies our assumption that $\lambda\to\infty$ corresponds to $R\to\infty$. Equation (24) provides the probability of finding a local Reynolds stress R, normalized by ξ_0, at $\mathbf{x}=\mathbf{x}_0$. Recall that $\xi_0 = -\partial_x \psi \partial_y \psi(\mathbf{x}_0)$ is local Reynolds stress associated with the modon solution, given by Eq. (12), and is therefore fixed for given parameters. Since we assumed that $F(t)=0$ as $t\to-\infty$, we can interpret Eq. (24) as a transition amplitude from an initial state, with no fluid motion, to final states with different values of R/ξ_0 for a given ξ_0. Interestingly, this PDF tail exhibits non-Gaussian behavior with a stretched exponential, which is enhanced over Gaussian. Thus, our simple calculation does reveal intermittency manifested in the PDF tail. Note that in the absence of forcing (i.e., $\kappa_0\to 0$), $P\to 0$. This is simply because the instanton cannot form without the forcing. Note also that Eqs. (22) and (24) imply that the more the instanton is localized in time (i.e., as $\gamma\to\infty$), the more rapidly the PDF decays for large R.

Now, upon using the relation $\lambda\xi_0 q = i(R/\xi_0)^{1/2}$ satisfied for the saddle point, F_0 reduces to the following form:

$$F_0 = 1 - \left(\frac{R}{\xi_0}\right)^{1/2}. \tag{25}$$

That is, F_0 is real, ensuring F to be a physical (observable) quantity. On the other hand, in the case $R/\xi_0 < 0$, the saddle-point solution does not lead to a physical solution. In other words, it is unlikely to have an instanton which has an opposite sign of Reynolds stress to the modon.

IV. DISCUSSION AND CONCLUSIONS

We have presented first results for the calculation of the tail of local Reynolds stress (vorticity flux) PDF in forced Hasegawa–Mima turbulence. Based on the observation that the PDF tail is governed by the bursty events associated with the appearance of coherent structures, the key idea was (1) to relate the bursty events as the creation of a coherent structure, say, a modon in the present paper and then (2) to envision the PDF tails as the transition amplitude from an initial state, with no fluid motion, to final states governed by the modon with different amplitudes in the long time limit.

The PDF was first formally expressed in terms of a path integral, by exploiting the Gaussian statistics of an external forcing. According to our expectation that the tail of PDF is related to the creation of a modon, an optimum path (among

all the paths) capturing this process was then found by a saddle-point method, with the ansatz that the saddle-point solution (instanton) is a temporally localized modon with a given radius. From this instanton solution, we found that the tail of the Reynolds stress (R) PDF deviates from Gaussian with the specific form $\exp[-cR^{3/2}]$, where c is a constant. Therefore, our simple model calculation reveals the intermittency of the PDF tails. While the non-Gaussian behavior may be generic for PDF tail, its precise scaling (i.e., exponent of R) may depend on temporal correlation of the forcing, which was chosen to be delta correlated in time, as well as possibly on the form of spatial correlation. Furthermore, the presence of other coherent structures may also lead to a different scaling of the tail of the PDF (thus, different intermittency).

In view of the simplicity of our model, a few remarks on the possible extension and improvement seem to be in order. First, in the present work, the global momentum flux (Reynolds stress) vanishes identically due to the spatial symmetry of a modon. This is why the PDF for the local Reynolds stress was considered in the present paper. A simple way of extending this model to study a global momentum flux PDF would be to introduce asymmetry in a system by assuming a large-scale shear or profile structure. The presence of shear flows (such as zonal flows) may, however, lead to the break-up of a dipole into monopole vortex.[18] Second, while an instanton here refers to the creation of a modon, the opposite process for the decay of modon can also be at work, which we called an anti-instanton. Then, multi-instantons, for instance, the time sequence-like instanton, anti-instanton, and instanton, may be present in a system, and their contribution to PDF tails can be calculated through a similar analysis. Third, if analytic form of other coherent structures (e.g., monopole and other multipole) is available, one could incorporate them in the computation of PDF tails as well. Fourth, it will be interesting to look at the PDF of the distribution of modon size itself, rather than taking the modon size as given. Finally, to address the particle or thermal flux PDF, the present model needs be extended to a more complicated one, such as the Hasegawa–Wakatani,[5] ITG model,[6] or dissipative trapped ion convective cell (DTICC) model.[7] These issues will be studied in future papers. Among these, the first three are expected to be rather straightforward while the last one would require a substantial work.

V. COMMENTS ON CALCULATIONS USING THE INSTANTON METHOD

In this work, like in Burgers turbulence,[11] an exact solution of a nonlinear equation had to be known in order to make progress. In other words, some information on the spatial form of coherent structures, by analytical calculation, numerical simulation, or intuition, should be available in order for the instanton method to be fruitful. That is, it seems almost impossible, if not very difficult, to use this method in the case where there is little information about nonlinear solution. Also, in realistic cases, a variety of structures and structure scales are likely to participate in the turbulence intermittency. Furthermore, even if a coherent structure solution is known, this method may not still work. As an example, in Burgers turbulence, the left tail of the PDF for the velocity difference is well understood to be due to shocks. Yet, the left tail of the PDF does not seem to be amenable to the instanton method. One of the mathematical routes leading to its failure is the inapplicability of a saddle-point method for the computation of a path integral, in which case the latter may not analytically be performed. For instance, in the present model, this may happen if the limit of large λ does not coincide with a large R limit. Finally, we recall that this method is likely to lead to the exponential dependence of PDF tails. Thus, it is not clear whether the issue of finite size scaling,[19] which requires a power-law PDF, can be addressed in this framework.

[1] P. A. Politzer, Phys. Rev. Lett. **84**, 1192 (2000); P. Beyer, S. Benkadda, X. Garbet, and P. H. Diamond, *ibid*. **85**, 4892 (2000); J. F. Drake, P. N. Guzdar, and A. B. Hassam, *ibid*. **61**, 2205 (1988).

[2] P. Bak, C. Tang, and K. Wiesenfeld, Phys. Rev. Lett. **59**, 381 (1987); P. H. Diamond and T. S. Hahm, Phys. Plasmas **2**, 3640 (1995).

[3] B. A. Carreras, B. van Milligen, C. Hidalgo *et al*., Phys. Rev. Lett. **83**, 3653 (1999).

[4] A. Hasegawa and K. Mima, Phys. Rev. Lett. **39**, 205 (1977).

[5] A. Hasegawa and M. Wakatani, Phys. Rev. Lett. **59**, 1581 (1987).

[6] B. G. Hong, F. Romanelli, and M. Ottaviani, Phys. Fluids B **3**, 615 (1991).

[7] P. H. Diamond, and H. Biglari, Phys. Rev. Lett. **65**, 2865 (1990).

[8] V. D. Larichev and G. M. Reznik, Dokl. Akad. Nauk SSSR **231**, 1077 (1976).

[9] H. W. Wyld, Ann. Phys. (N.Y.) **14**, 143 (1961).

[10] J. Zinn-Justin, *Field Theory and Critical Phenomena* (Clarendon, Oxford, 1989).

[11] V. Gurarie and A. Migdal, Phys. Rev. E **54**, 4908 (1996).

[12] G. Falkovich, I. Kolokolov, V. Lebedev, and A. Migdal, Phys. Rev. E **54**, 4896 (1996).

[13] E. Balkovsky, G. Falkovich, I. Kolokolov, and V. Lebedev, Phys. Rev. Lett. **78**, 1452 (1997).

[14] S. Coleman, *Aspects of Symmetry* (Cambridge University Press, Cambridge, 1985).

[15] G. 't Hooft, Phys. Rev. Lett. **37**, 8 (1976); Phys. Rev. D **14**, 3432 (1976).

[16] J. Fleischer and P. H. Diamond, Phys. Lett. A **283**, 237 (2001).

[17] P. C. Martin, E. D. Sigga, and H. A. Rose, Phys. Rev. E **8**, 423 (1973).

[18] W. Horton, T. Tajima, and T. Kamimura, Phys. Fluids **30**, 3485 (1987).

[19] C. Hidalgo, M. A. Pedrose, J. Castellano *et al*., "On the radial scale of fluctuations in the JT-III stellarator," Plasma Phys. Control. Fusion (in press).